Outage Probability of Two-Way Full-Duplex Relay System With Hardware Impairments

Xuan Nam Tran*, Ba Cao Nguyen*, Dinh Tan Tran†
* Le Quy Don Technical University, Hanoi, Vietnam (e-mail: namtx@mta.edu.vn, bacao.sqtt@gmail.com)
† Telecommunication University, Nha Trang, Vietnam (e-mail:trdinhtan@gmail.com)

***Abstract*—In this paper, we analyze performance of a full-duplex (FD) decode-and-forward (DF) two-way relay system, where two terminal nodes exchange information via a relay node over a same frequency band and time slot. Unlike previous works on two-way full-duplex relay systems, we consider a system which is affected by both hardware impairments and residual interference due to imperfect self-interference cancellation (SIC) at the full-duplex nodes. We derive exact outage probability based on the signal to interference plus noise and distortion ratio of the considered system. Our analysis based on numerical results show significant performance degradation due to transceiver impairments. The outage probability is caused to fall to an irreducible floor even at low residual self-interference. Finally, Monte Carlo simulations are also used to validate numerical results.**

***Index Terms*—Full-duplex two-way relay, self-interference cancellation, decode-and-forward, outage probability, hardware impairments.**

I. Introduction

With the fast development of advanced wireless technology, the demand for high-rate data transmission over a limited spectrum has prompted researchers and network designers to move from one-way relay systems to two-way relay (TWR) ones. Moreover, in-band full-duplex (IBFD) radio technology has matured for possible implementation in the next generation of wireless communications [1], [2]. The combination of IBFD technology with TWR systems provides a IBFD-TWR system that enables high data rate transmission and spectral efficiency improvement [3]–[6]. However, performance of IBFD-TWR systems is significantly affected by the residual self-interference (RSI) due to imperfect self-interference cancellation (SIC) [7]–[9].

Various works have focused on analyzing and proposing solutions to improve performance of IBFD-TWR systems in the case of imperfect SIC. In [3] the outage probability (OP) of a IBFD-TWR system, which used amplify-and-forward (AF) protocol, was derived for the case of perfect and imperfect channel state information (CSI). This work showed that the OP of the IBFD-TWR system soon exhibits an error floor at the high signal to noise ratio (SNR) region due to imperfect CSI. In [4] an IBFD-TWR system using AF relaying was analyzed and optimized for the case of multiple relays. The authors was successful in deriving the OP, bit error rate (BER) and ergodic capacity of the system. The paper also demonstrated that the IBFD-TWR system has higher efficiency and better performance than a half-duplex (HD) TWR system when the RSI is sufficiently small. In other works [10], [11], multiple relays were proposed to improve the system performance of the IBFD-TWR AF systems.

Besides the AF protocol, decode-and-forward (DF) relaying was also widely investigated for the IBFD-TWR system in the literature. In the two early works in [5] and [6], the OP was evaluated for an IBFD-TWR system using DF relaying. The authors obtained the OP for seven different cases corresponding to different power allocation factors at the relay. They also analyzed the OP for the symmetrical and asymmetrical model. The results of these papers demonstrated that the IBFD-TWR DF systems also suffer from an outage floor at the high power region due to the RSI incurred by the IBFD mode. In a next work [12], outage performance of the IBFD-TWR DF system was analyzed for the case with both imperfect CSI and imperfect SIC. In the recent researches, performance of the IBFD-TWR system was further explored for the case with cooperative communication, and energy harvesting in [13]–[15].

It is noted from the above discussion that while performance of the IBFD-TWR systems was widely studied in the literature the previous works only considered the case with ideal hardware. In practice, the system hardware is not perfectly manufactured and often affected by different factors, such as manufacturing errors, phase oscillator noises, I/Q modulation imbalance, nonlinear distortion of the high power amplifier (HPA) at the transmitter and the low noise amplifier (LNA) at the receiver. These imperfect factors were demonstrated to further deteriorate the system performance and also cause an outage floor [16]–[18].

In this paper, we intent to carry out a performance analysis of the IBFD-TWR DF system in a more realistic hardware impairment conditions. We also use outage probability to evaluate and analyze the system performance and compare it with that of the ideal hardware systems in [5], [6]. Compared with the previous works, our contributions can be summarized as follows:

– We consider an IBFD-TWR DF system that is close to a realistic system with an aggregate impact of transceiver hardware and the imperfect SIC at all nodes (the terminal nodes and the relay node).

– We derive the exact expressions of the Signal to Interference plus Noise and Distortion Ratio (SINDR) for all related links in the system. Based on these SINDRs, a new closed-form expression of the outage probability of the system for seven different cases according to the power allocation factor at the relay node is obtained. Unlike the previous works in [5], [6], [12], [19], which analyzed the OP while taking into account the effect of imperfect SIC or transmit power at only the relay, we consider a system with imperfect SIC at all nodes together with the RSI at the FD nodes. Moreover, we determine the OP according to the average SNR of the system.

– Based on the mathematical results, we analyze the system performance under the impact of both HI and RSI. We show that the OP of the considered system have an outage floor at the high SNR regime. Finally, we validate the numerical results by Monte-Carlo simulations.

The rest of the paper is organized as follows: Section II presents the system model. Section III focuses on analyzing the outage probability of considered system. Numerical results and discussion are discussed in Section IV and finally, Section V draws the conclusion of the paper.

II. System Model

To derive the model of IBFD-TWR DF system with hardware impairments (HI), we begin with a simple model having a transmitter and a receiver. Each of these two nodes has an antenna which is used for both transmission and reception. Thus, we have a single link between the the transmitter and the receiver. In the case of HI system, the received signal at the receiver via a single link from the transmitter to the receiver is given by [17]

$$y = h(x + \eta) + z, \tag{1}$$

where x is the intended signal at the transmitter; η describes HI at both the transmitter and the receiver with $\eta \sim \mathcal{CN}(0, k^2 P)$; k is the aggregate level of impairments with the exact contribution from the transmitter hardware and the receiver hardware; h is the coupling coefficient of the link from the transmitter to the receiver; z is the Additive White Gaussian Noise (AWGN) with zero-mean and variance of σ^2, i.e. $z \sim \mathcal{CN}(0, \sigma^2)$ at the receiver. Based on this assumption, we derive a new model of IBFD-TWR DF system with hardware impairments as in Fig. 1.

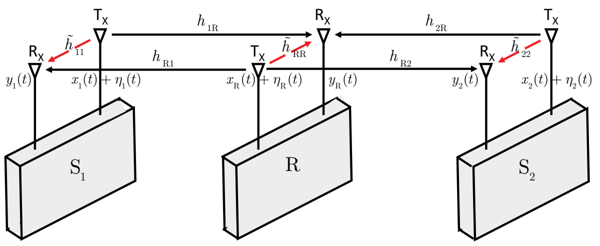

Figure 1. Block diagram of the IBFD-TWR DF system with transceiver impairments.

Data is transmitted from node S_1 to node S_2 via a relay node R and vice versa. At time slot t, the received signal at the relay node is given by:

$$y_{\mathrm{R}}(t) = h_{1\mathrm{R}}\tilde{x}_1(t) + h_{2\mathrm{R}}\tilde{x}_2(t) + \tilde{h}_{\mathrm{RR}}\tilde{x}_{\mathrm{R}}(t) + z_{\mathrm{R}}(t), \tag{2}$$

where $\tilde{x}_1(t) \triangleq x_1(t) + \eta_1(t)$; $\tilde{x}_2(t) \triangleq x_2(t) + \eta_2(t)$; $\tilde{x}_{\mathrm{R}}(t) \triangleq x_{\mathrm{R}}(t) + \eta_{\mathrm{R}}(t)$, with $x_1(t)$, $x_2(t)$, and $x_{\mathrm{R}}(t)$ being the desired transmitted signals of the nodes S_1, S_2 and R, respectively; $\tilde{x}_1(t)$, $\tilde{x}_2(t)$ and $\tilde{x}_{\mathrm{R}}(t)$ are the actual transmitted signals from nodes S_1, S_2 and R; $\eta_1(t)$, $\eta_2(t)$ and $\eta_{\mathrm{R}}(t)$ are the distortions caused by transmitting and receiving parts because of the nodes S_1, S_2 and R, with $\eta_1 \sim \mathcal{CN}(0, k_1^2 P_1)$, $\eta_2 \sim \mathcal{CN}(0, k_2^2 P_2)$ and $\eta_{\mathrm{R}} \sim \mathcal{CN}(0, k_{\mathrm{R}}^2 P_{\mathrm{R}})$; where P_i is the transmit power and k_i indicates the impact level of device hardware impairments, $i = 1, 2, \mathrm{R}$ corresponding to the node S_1, S_2 and R; $h_{1\mathrm{R}}$, $h_{2\mathrm{R}}$ and $\tilde{h}_{\mathrm{RR}}$ are the fading coefficients of channels from S_1, S_2 to R and from the transmitting antenna to the receiving antenna of R; $z_{\mathrm{R}}(t)$ is the AWGN with $z_{\mathrm{R}} \sim \mathcal{CN}(0, \sigma_{\mathrm{R}}^2)$. When $k_1 = k_2 = k_{\mathrm{R}} = 0$ this system becomes an ideal hardware system.

At the same time slot t, the relay R transmits the re-encoded signal to S_1, S_2, which is based on the previously received signal. The received signal at S_1, S_2 are given by, respectively:

$$y_1(t) = h_{\mathrm{R}1}\tilde{x}_{\mathrm{R}}(t) + \tilde{h}_{11}\tilde{x}_1(t) + z_1(t), \tag{3}$$

$$y_2(t) = h_{\mathrm{R}2}\tilde{x}_{\mathrm{R}}(t) + \tilde{h}_{22}\tilde{x}_2(t) + z_2(t), \tag{4}$$

where $h_{\mathrm{R}1}$, $h_{\mathrm{R}2}$, $\tilde{h}_{11}$, $\tilde{h}_{22}$ are the fading coefficients of the links from R to S_1, from R to S_2 and from transmitting antenna to receiving antenna of S_1, S_2, respectively. It is noted that, $|h_{\mathrm{R}2}|^2 = |h_{2\mathrm{R}}|^2$, $|h_{\mathrm{R}1}|^2 = |h_{1\mathrm{R}}|^2$; $z_i(t)$ is the AWGN, $z_i \sim \mathcal{CN}(0, \sigma_i^2)$, $i = 1, 2$.

The transmitted signal $\tilde{x}_{\mathrm{R}}(t)$ at R consists of two signals $\bar{x}_1(t)$ and $\bar{x}_2(t)$, (e.g., $\tilde{x}_{\mathrm{R}}(t) = \bar{x}_1(t) + \bar{x}_2(t) + \eta_{\mathrm{R}}(t)$) contains the same information with two previous received signals $x_1(t-1)$ and $x_2(t-1)$, but were re-encoded with different power allocation levels, $\mathbb{E}\{|\bar{x}_1(t)|^2\} = (1-\lambda)P_{\mathrm{R}}$, $\mathbb{E}\{|\bar{x}_2(t)|^2\} = \lambda P_{\mathrm{R}}$, such as $\lambda \in (0, 1)$. Using the network coding technique [4], S_1 and S_2 can be totally subtracted from the components being transmitted before, therefore we have:

$$y_1(t) = h_{\mathrm{R}1}[\bar{x}_2(t) + \eta_{\mathrm{R}}(t)] + \tilde{h}_{11}\tilde{x}_1(t) + z_1(t), \tag{5}$$

$$y_2(t) = h_{\mathrm{R}2}[\bar{x}_1(t) + \eta_{\mathrm{R}}(t)] + \tilde{h}_{22}\tilde{x}_2(t) + z_2(t). \tag{6}$$

It is noted that, in this paper, we assume that the three nodes in this system can combine all techniques of SIC, after SIC, the RSIs denoted by I_i can be modeled by a complex Gaussian distributed random variable [3]–[5] with zero-mean and variance $\sigma_{\mathrm{RSI}_i}^2 = \tilde{\Omega}_i P_i$, where $\tilde{\Omega}_i$ denotes the SIC capability of the FD node $i, i = 1, 2, \mathrm{R}$. Therefore, equations (2), (5), (6) can be rewritten as follows:

$$y_{\mathrm{R}}(t) = h_{1\mathrm{R}}\tilde{x}_1(t) + h_{2\mathrm{R}}\tilde{x}_2(t) + I_{\mathrm{R}} + z_{\mathrm{R}}(t), \tag{7}$$

$$y_1(t) = h_{\mathrm{R}1}[\bar{x}_2(t) + \eta_{\mathrm{R}}(t)] + I_1 + z_1(t), \tag{8}$$

$$y_2(t) = h_{\mathrm{R}2}[\bar{x}_1(t) + \eta_{\mathrm{R}}(t)] + I_2 + z_2(t). \tag{9}$$

From (7), (8), (9), the SINDR for the IBFD-TWR DF system are given by:

$$\gamma_{\mathrm{S}_1\mathrm{R}} = \frac{\rho_1 P_1}{\sigma_{\mathrm{R}}^2 + \sigma_{\mathrm{RSI_R}}^2 + \rho_1 k_1^2 P_1 + \rho_2 k_2^2 P_2}, \tag{10}$$

$$\gamma_{\mathrm{S}_2\mathrm{R}} = \frac{\rho_2 P_2}{\sigma_{\mathrm{R}}^2 + \sigma_{\mathrm{RSI_R}}^2 + \rho_1 k_1^2 P_1 + \rho_2 k_2^2 P_2}, \tag{11}$$

$$\gamma_{\mathrm{RS}_1} = \frac{\rho_1 \lambda P_{\mathrm{R}}}{\sigma_1^2 + \sigma_{\mathrm{RSI}_1}^2 + \rho_1 k_{\mathrm{R}}^2 P_{\mathrm{R}}}, \tag{12}$$

$$\gamma_{\mathrm{RS}_2} = \frac{\rho_2(1-\lambda)P_{\mathrm{R}}}{\sigma_2^2 + \sigma_{\mathrm{RSI}_2}^2 + \rho_2 k_{\mathrm{R}}^2 P_{\mathrm{R}}}, \tag{13}$$

$$\gamma_{\mathrm{sum}} = \frac{\rho_1 P_1 + \rho_2 P_2}{\sigma_{\mathrm{R}}^2 + \sigma_{\mathrm{RSI_R}}^2 + \rho_1 k_1^2 P_1 + \rho_2 k_2^2 P_2}, \tag{14}$$

where $\rho_1 = |h_1|^2 = |h_{\mathrm{R1}}|^2 = |h_{1\mathrm{R}}|^2$; $\rho_2 = |h_2|^2 = |h_{\mathrm{R2}}|^2 = |h_{2\mathrm{R}}|^2$; $\gamma_{\mathrm{S_1R}}$, $\gamma_{\mathrm{S_2R}}$, $\gamma_{\mathrm{RS_1}}$, $\gamma_{\mathrm{RS_2}}$ represent the SINDR of the communication links from S_1 and S_2 to R, from R to S_1 and S_2, respectively; γ_{sum} represents the SINDR of the superimposed signal at the relay node.

III. Performance Analysis

Outage probability of a random link between S_1, R, S_2 can be defined as folllows:

$$\mathcal{P}_{\mathrm{out}} = \Pr\{C_j < \mathcal{R}_j\}, \tag{15}$$

where $C_j = \log_2(1+\gamma_j)$; γ_j, $\mathcal{R}_j$ are the SINDR and the minimum required data rate of link j, $j = 1, 2$. The outage occurs when

$$\log_2(1+\gamma_{\mathrm{S_1R}}) < \mathcal{R}_1 \text{ or } \log_2(1+\gamma_{\mathrm{RS_2}}) < \mathcal{R}_1, \tag{16}$$

$$\log_2(1+\gamma_{\mathrm{S_2R}}) < \mathcal{R}_2 \text{ or } \log_2(1+\gamma_{\mathrm{RS_1}}) < \mathcal{R}_2, \tag{17}$$

$$\log_2(1+\gamma_{\mathrm{sum}}) < \mathcal{R}_1 + \mathcal{R}_2. \tag{18}$$

Thereby, we have:

$$\gamma_{\mathrm{S_1R}} < 2^{\mathcal{R}_1} - 1 \text{ or } \gamma_{\mathrm{RS_2}} < 2^{\mathcal{R}_1} - 1, \tag{19}$$

$$\gamma_{\mathrm{S_2R}} < 2^{\mathcal{R}_2} - 1 \text{ or } \gamma_{\mathrm{RS_1}} < 2^{\mathcal{R}_2} - 1, \tag{20}$$

$$\gamma_{\mathrm{sum}} < 2^{\mathcal{R}_1+\mathcal{R}_2} - 1. \tag{21}$$

Denote $x = 2^{\mathcal{R}_1} - 1$, $y = 2^{\mathcal{R}_2} - 1$, it therefore follows that $2^{\mathcal{R}_1+\mathcal{R}_2} - 1 = x + y + xy$, thereby we can determine the outage probability as follows: $\mathcal{P}_{\mathrm{out}} = \Pr\{\mathcal{A} \cup \mathcal{B} \cup \mathcal{C}\}$, where the events $\mathcal{A}, \mathcal{B}, \mathcal{C}$ are defined as the following expression: $\mathcal{A} = (\gamma_{\mathrm{S_1R}} < x) \cup (\gamma_{\mathrm{RS_1}} < y), \mathcal{B} = (\gamma_{\mathrm{S_2R}} < y) \cup (\gamma_{\mathrm{RS_2}} < x), \mathcal{C} = (\gamma_{\mathrm{sum}} < z)$,with $z = x + y + xy$.

It is noted that all the analysis in this paper is applied for Rayleigh fading channel. Assume Rayleigh fading and that the relay node knows the global CSI to decode the received signal successfully and the terminal nodes know partial CSI to subtract the transmitted signals in advance.

Theorem: Under the Rayleigh fading channel and hardware impairments, we can determine the exact outage probability expression for the following seven cases:

$$\mathcal{P}_{\mathrm{out}} = \begin{cases} 1 - Q_2 Q_3, & \text{case } 1, \\ 1 - Q_2 Q_3 Q_5, & \text{case } 2, \\ 1 - Q_1 Q_3 Q_5, & \text{case } 3, \\ 1 - Q_2 Q_4 Q_5, & \text{case } 4, \\ 1 - Q_2 Q_4, & \text{case } 5, \\ 1 - Q_1 Q_4 Q_5, & \text{case } 6, \\ 1 - Q_1 Q_4, & \text{case } 7, \end{cases} \tag{22}$$

where

$$Q_1 = \frac{a_{12}}{a_{12}+b_{12}} \exp\Big(-\frac{x t_{\mathrm{R}}}{a_{12}}\Big), \tag{23}$$

$$Q_2 = \exp\Big(-\frac{y t_1}{c_{12}}\Big)\Big[1 - \frac{b_{12}}{a_{12}+b_{12}} \exp\Big(\frac{x t_{\mathrm{R}} c_{12} - y t_1 a_{12}}{b_{12} c_{12}}\Big)\Big], \tag{24}$$

$$Q_3 = \frac{a_{34}}{a_{34}+b_{34}} \exp\Big(-\frac{y t_{\mathrm{R}}}{a_{34}}\Big), \tag{25}$$

$$Q_4 = \exp\Big(-\frac{x t_2}{c_{34}}\Big)\Big[1 - \frac{b_{34}}{a_{34}+b_{34}} \exp\Big(\frac{y t_{\mathrm{R}} c_{34} - x t_2 a_{34}}{b_{34} c_{34}}\Big)\Big], \tag{26}$$

$$Q_5 = \begin{cases} \frac{a_5}{a_5-b_5}\exp(-\frac{z t_{\mathrm{R}}}{a_5}), \text{ when } 1-k_1^2 z \leqslant 0 \ \& \ 1-k_2^2 z > 0, \\ \frac{b_5}{b_5-a_5}\exp(-\frac{z t_{\mathrm{R}}}{b_5}), \text{ when } 1-k_1^2 z > 0 \ \& \ 1-k_2^2 z \leqslant 0, \\ \frac{a_5}{a_5-b_5}\exp(-\frac{z t_{\mathrm{R}}}{a_5}) + \frac{b_5}{b_5-a_5}\exp(-\frac{z t_{\mathrm{R}}}{b_5}), \\ \qquad \text{when } 1-k_1^2 z > 0 \ \& \ 1-k_2^2 z > 0 \ \& \ a_5 \neq b_5, \\ (1+\frac{z t_{\mathrm{R}}}{a_5})\exp(-\frac{z t_{\mathrm{R}}}{a_5}), \\ \qquad \text{when } 1-k_1^2 z > 0 \ \& \ 1-k_2^2 z > 0 \ \& \ a_5 = b_5, \end{cases} \tag{27}$$

where $a_{12} = \Omega_1 P_1 (1-k_1^2 x)$, $b_{12} = \Omega_2 P_2 k_2^2 x$, $c_{12} = \Omega_1 P_{\mathrm{R}}(\lambda - k_{\mathrm{R}}^2 y)$, $a_{34} = \Omega_2 P_2 (1-k_2^2 y)$, $b_{34} = \Omega_1 P_1 k_1^2 y$, $c_{34} = \Omega_2 P_{\mathrm{R}}(1-\lambda-k_{\mathrm{R}}^2 x)$, $a_5 = \Omega_2 P_2 (1-k_2^2 z)$, $b_5 = \Omega_1 P_1 (1-k_1^2 z)$, $t_1 = \sigma_1^2 + \sigma_{\mathrm{RSI}_1}^2$, $t_2 = \sigma_2^2 + \sigma_{\mathrm{RSI}_2}^2$, $t_{\mathrm{R}} = \sigma_{\mathrm{R}}^2 + \sigma_{\mathrm{RSI_R}}^2$.

The above seven cases of the above OP are defined according to the power allocation factor in Table I below.

Table I
POWER ALLOCATION SCHEME

Case	Power allocation factor λ	Outage links
1	$(k_{\mathrm{R}}^2 y, \min\{X, Z\})$	$\mathrm{R} \to \mathrm{S}_1$, $\mathrm{S}_1 \to \mathrm{R}$, $\mathrm{S}_2 \to \mathrm{R}$
2	$(X, \min\{Y, Z\})$	$\mathrm{R} \to \mathrm{S}_1$, $\mathrm{S}_1 \to \mathrm{R}$, $\mathrm{S}_2 \to \mathrm{R}$, $\mathrm{R_{sum}}$
3	(Y, Z)	$\mathrm{S}_1 \to \mathrm{R}$, $\mathrm{S}_2 \to \mathrm{R}$, $\mathrm{R_{sum}}$
4	$\begin{pmatrix} \max\{k_{\mathrm{R}}^2 y, Z\}, \\ \min\{1-k_{\mathrm{R}}^2 x, Y\} \end{pmatrix}$	$\mathrm{R} \to \mathrm{S}_1$, $\mathrm{S}_1 \to \mathrm{R}$, $\mathrm{R} \to \mathrm{S}_2$, $\mathrm{S}_2 \to \mathrm{R}$, $\mathrm{R_{sum}}$
5	$\begin{pmatrix} \max\{k_{\mathrm{R}}^2 y, Z\}, \\ \min\{1-k_{\mathrm{R}}^2 x, Y\} \end{pmatrix}$	$\mathrm{R} \to \mathrm{S}_1$, $\mathrm{S}_1 \to \mathrm{R}$, $\mathrm{R} \to \mathrm{S}_2$, $\mathrm{S}_2 \to \mathrm{R}$
6	$(\max\{Y, Z\}, T)$	$\mathrm{S}_1 \to \mathrm{R}$, $\mathrm{R} \to \mathrm{S}_2$, $\mathrm{S}_2 \to \mathrm{R}$, $\mathrm{R_{sum}}$
7	$(\max\{Y, T\}, 1-k_{\mathrm{R}}^2 x)$	$\mathrm{S}_1 \to \mathrm{R}$, $\mathrm{R} \to \mathrm{S}_2$, $\mathrm{S}_2 \to \mathrm{R}$

$$X = k_{\mathrm{R}}^2 y + \frac{P_1 t_1 y[1-k_2^2 y - k_1^2(z-y)]}{P_{\mathrm{R}} t_{\mathrm{R}} (z-y)},$$
$$Y = k_{\mathrm{R}}^2 y + \frac{P_1 t_1 y(1-k_1^2 x)}{P_{\mathrm{R}} t_{\mathrm{R}} x},$$
$$Z = 1 - k_{\mathrm{R}}^2 x - \frac{P_2 t_2 x(1-k_2^2 y)}{P_{\mathrm{R}} t_{\mathrm{R}} y},$$
$$T = 1 - k_{\mathrm{R}}^2 x - \frac{P_2 t_2 x[1-k_1^2 x - k_2^2(z-x)]}{P_{\mathrm{R}} t_{\mathrm{R}} (z-x)}.$$

Proof:

1) When $1-k_1^2 x \leqslant 0$ or $\lambda - k_{\mathrm{R}}^2 y \leqslant 0$ or $1-\lambda-k_{\mathrm{R}}^2 x \leqslant 0$ or $1-k_2^2 y \leqslant 0$ or $(1-k_1^2 z \leqslant 0 \ \& \ 1-k_2^2 z \leqslant 0)$, at least one of five cases in (19), (20) and (21) always occurs, therefore OP = 1.

2) When all conditions in 1) do not occur simultaneously, we can determine the OP as follows: set $\mathcal{P}_{\mathrm{out}_{12}} = \Pr\{\mathcal{A}\}$, $\mathcal{P}_{\mathrm{out}_{34}} = \Pr\{\mathcal{B}\}$, $\mathcal{P}_{\mathrm{out}_5} = \Pr\{\mathcal{C}\}$ with the $\mathcal{A}, \mathcal{B}, \mathcal{C}$ events being defined as above. We have

$$\mathcal{P}_{\mathrm{out}_{12}} = \begin{cases} 1 - Q_1, \ \lambda \geqslant Y, \\ 1 - Q_2, \ \lambda < Y. \end{cases} \tag{28}$$

$$\mathcal{P}_{\text{out}_{34}} = \begin{cases} 1 - Q_3, \, \lambda \leqslant Z, \\ 1 - Q_4, \, \lambda > Z. \end{cases} \tag{29}$$

$$P_{\text{out}_5} = 1 - Q_5. \tag{30}$$

From these results, we can get the OP of the system as in equation (22). It is noted that for case 4 and case 5, there is a same selection range λ but for each specific value of λ, only one of the two cases occurs, depending on the value of the roots of the quadratic equation

$$a\lambda^2 + b\lambda + c = 0 \tag{31}$$

to determine exactly case 4 or case 5, where $a = P_{\text{R}} t_{\text{R}} z$, $b = P_2 t_2 x(1 - k_2^2 z) - P_1 t_1 y(1 - k_1^2 z) - P_{\text{R}} t_{\text{R}} z(1 - k_{\text{R}}^2 x + k_{\text{R}}^2 y)$, and $c = P_1 t_1 y(1 - k_1^2 z)(1 - k_{\text{R}}^2 x) - P_2 t_2 x k_{\text{R}}^2 y(1 - k_2^2 z) + P_{\text{R}} t_{\text{R}} z k_{\text{R}}^2 y(1 - k_{\text{R}}^2 x)$.

IV. Numerical Results and Discussions

In this section, we present numerical results to evaluate performance of the IBFD-TWR DF system. The analyzed results also validated using the Monte-Carlo simulations. We consider the impact of the HI and RSI on the system performance under the imperfect SIC by generating random channel response chains ρ_i with the mean values Ω_i, $i = 1, 2$. In this imperfect SIC scenario, performance of the HI system is compared with the ideal hardware system ($k_1 = k_2 = k_{\text{R}} = 0$) for different cases of the RSI. We also investigate the effect of the power allocation factor, HIs, and the RSI on the system performance.

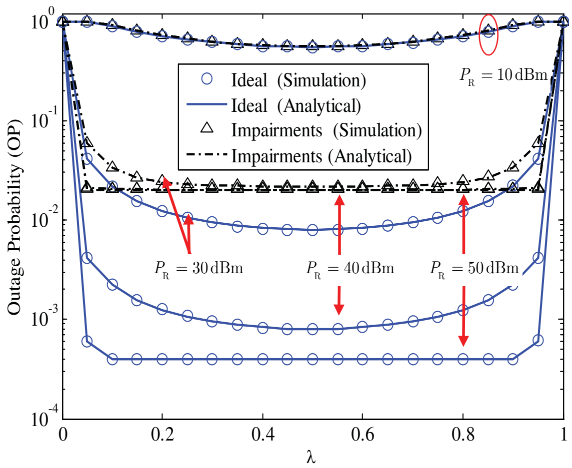

Figure 2. The OP of the symmetric model versus power allocation factor with several cases of difference transmit power at the relay node.

Fig. 2 shows the OP of the system versus the power allocation factor. The curves were generated by the analytical expressions in (22) and the marker symbols $\triangle$ and $\circ$ show the results of Monte-Carlo simulations, with $P_1 = P_2 = 40$ dBm, and varying P_{R} . The investigated threshold for the OP is set as $\mathcal{R}_1 = \mathcal{R}_2 = 1$ bit/s/Hz, from which we obtain $x = y = 2^1 - 1 = 1$ and $z = x + y + xy = 3$. The aggregate level of impairments is $k_1 = k_2 = k_{\text{R}} = 0.1$. The average channel gains are $\Omega_1 = \Omega_2 = 1$. The variance of the RSI is $\sigma_{\text{RSI}_1}^2 = \sigma_{\text{RSI}_2}^2 = \sigma_{\text{RSI}_{\text{R}}}^2 = 1$ and the variance of the AWGN is $\sigma_1^2 = \sigma_2^2 = \sigma_{\text{R}}^2 = 1$. The transmit power at the relay node is set as $P_{\text{R}} = 10, 30, 40,$ and 50 dBm. With these parameters the considered model becomes symmetrical, and it achieves the best performance when the relay node allocates its power equally to both sides ($\lambda = 0.5$). For example, when $P_{\text{R}} = 40$ dBm , we have $X = 0.495$; $Y = 1$; $Z = 0$; $T = 0.495$. Therefore, the value of λ in Table I is determined as follows: $(0.01, 0)$ for case 1; $(0.495, 0)$ for case 2; $(1, 0)$ for case 3; $(0.01, 0.99)$ for case 4 and 5; $(1, 0.495)$ for case 6; and $(1, 0.99)$ for case 7. Thus, there is only the range $(0.01, 0.99)$ which is suitable for λ and either case 4 or case 5 occurs. The result of equation (31) becomes $2\lambda^2 - 2\lambda + 0.9812 = 0$. Due to the fact that this equation has no real root, therefore, only case 5 occurs. It is also noted that the curves indicating the OP of the ideal hardware system in Fig. 2 are those for the case of imperfect SIC in Fig. 2 of [5] and Fig. 3 of [6] with $P_{\text{R}} = 30$, 40, 50 dBm. From Fig. 2, it is clear that when the transmit power at the relay node P_{R} is high enough, the system performance exhibits a saturated floor. At this saturation level although $P_{\text{R}} = 40$ dBm or $P_{\text{R}} = 50$ dBm, the system performance with HI does not change with λ . When the system performance becomes saturated, the ideal hardware system has the OP that is about 50 times less than the one of the HI system.

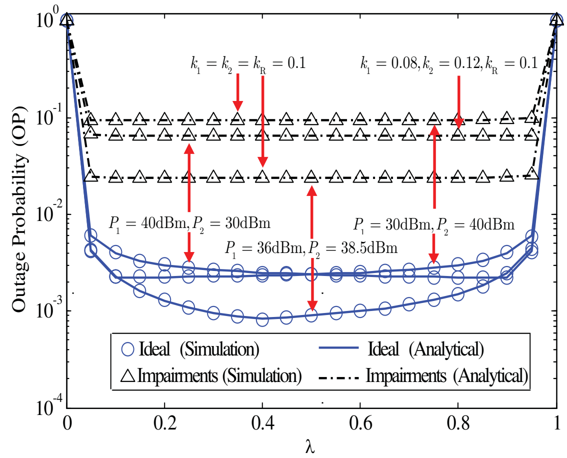

Figure 3. The OP of the asymmetric model versus power allocation factor with several cases of difference transmit power and distortion factor at the terminal nodes.

Fig. 3 illustrates the OP for an asymmetric model with $P_{\text{R}} = 40$ dBm. The threshold, the RSI and the variance of the AWGN are the same as used in Fig. 2. The transmit power and distortion factor at the two terminal nodes are changed. In Fig. 3 when the difference between the two terminal nodes is smaller, the system performance is higher. With the distortion factor $k_1 = k_2 = k_{\text{R}} = 0.1$ and the total transmit power at the two terminal nodes $P_1 + P_2 = 11$W, when the difference is small ($P_1 = 36$ dBm (4W), $P_2 = 38.5$dBm (7W)), the system performance is much better than that of the case with large difference ($P_1 = 30$ dBm (1W), $P_2 = 40$ dBm (10W) or $P_1 = 40$ dBm, $P_2 = 30$ dBm). When the evaluation parameter at the relay node, and also the transmit power and the distortion factor at the two terminal nodes are simultaneously changed as $P_1 = 40$ dBm, $P_2 = 30$ dBm, and $k_1 = 0.08$, $k_2 = 0.12$, the system performance for the case with HI is improved in comparison with the case of

$k_1 = k_2 = 0.1$. This is because when the transmit power increases, the distortion factor decreases at node S_1 and the transmit power decreases, the distortion factor at the node S_2 increases, therefore the impact of the HI is decreased.

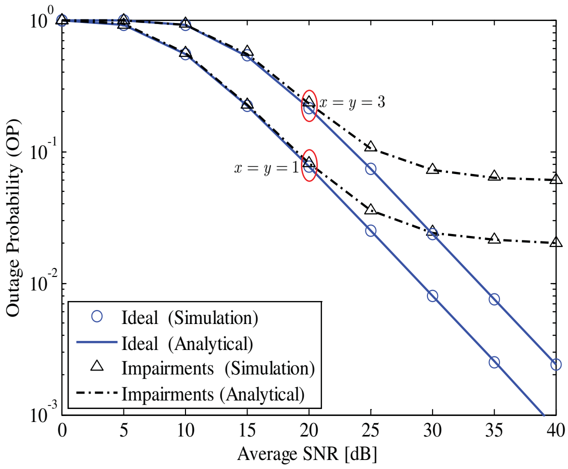

Figure 4. The OP of the system following SNR with the fixed distortion factor and RSI.

Fig. 4 plots the OP of the system versus the average SNR, with $\mathrm{SNR} = \frac{\Omega_i P_i}{\sigma_i^2}, i = 1, 2, \mathrm{R}$. In Fig. 4 the RSI and the hardware impairment levels are fixed with $\sigma^2_{\mathrm{RSI}_1} = \sigma^2_{\mathrm{RSI}_2} = \sigma^2_{\mathrm{RSI}_\mathrm{R}} = 1, k_1 = k_2 = k_\mathrm{R} = 0.1$, $\lambda = 0.5$. Fig. 4 again shows the apparent impact of HI on the system performance. With the selected parameters, when $\mathrm{SNR} > 20$ dB the system performance of the case with HI slightly increases and reaches the outage floor when $\mathrm{SNR} = 40$ dB. For the ideal hardware system, the floor effect appears with the higher SNR regime.

V. Conclusion

Hardware impairments always occur in radio devices due to imperfect manufacturing. Therefore, it is always desired to evaluate performance of wireless systems with HI. However, due to mathematical complication, the study of HI impact is often overlooked, especially for IBFD-TWR systems. In this paper, we have analyzed the impacts of both hardware impairments and RSI on the performance of the IBFD-TWR DF system. We have obtained the exact expression for the system OP and evaluated the impact of HI and RSI on the system performance to overcome the limitations of the previous related works. Analysis results are an important reference in the practical full-duplex relay system deployment and exploitation.

References

[1] I. Ahmed, H. Khammari, A. Shahid, A. Musa, K. S. Kim, E. De Poorter, and I. Moerman, "A survey on hybrid beamforming techniques in 5g: Architecture and system model perspectives," *IEEE Communications Surveys & Tutorials*, 2018.

[2] Z. Wei, X. Zhu, S. Sun, Y. Jiang, A. Al-Tahmeesschi, and M. Yue, "Research issues, challenges, and opportunities of wireless power transfer-aided full-duplex relay systems," *IEEE Access*, vol. 6, pp. 8870–8881, 2018.

[3] D. Choi and J. H. Lee, "Outage probability of two-way full-duplex relaying with imperfect channel state information," *IEEE Communications Letters*, vol. 18, no. 6, pp. 933–936, June 2014.

[4] H. Cui, M. Ma, L. Song, and B. Jiao, "Relay selection for two-way full duplex relay networks with amplify-and-forward protocol," *IEEE Transactions on Wireless Communications*, vol. 13, no. 7, pp. 3768–3777, July 2014.

[5] C. Li, Y. Wang, Z. Chen, Y. Yao, and B. Xia, "Performance analysis of the full-duplex enabled decode-and-forward two-way relay system," in *2016 IEEE International Conference on Communications Workshops (ICC)*, May 2016, pp. 559–564.

[6] C. Li, Z. Chen, Y. Wang, Y. Yao, and B. Xia, "Outage analysis of the full-duplex decode-and-forward two-way relay system," *IEEE Transactions on Vehicular Technology*, vol. 66, no. 5, pp. 4073–4086, May 2017.

[7] S. Hong, J. Brand, J. I. Choi, M. Jain, J. Mehlman, S. Katti, and P. Levis, "Applications of self-interference cancellation in 5g and beyond," *IEEE Communications Magazine*, vol. 52, no. 2, pp. 114–121, 2014.

[8] B. C. Nguyen, X. N. Tran, and D. T. Tran, "Performance analysis of in-band full-duplex amplify-and-forward relay system with direct link," in *Recent Advances in Signal Processing, Telecommunications & Computing (SigTelCom), 2018 2nd International Conference on*. IEEE, 2018, pp. 192–197.

[9] K. Yang, H. Cui, L. Song, and Y. Li, "Efficient full-duplex relaying with joint antenna-relay selection and self-interference suppression," *IEEE Transactions on Wireless Communications*, vol. 14, no. 7, pp. 3991–4005, July 2015.

[10] P. Xing, J. Liu, C. Zhai, X. Wang, and X. Zhang, "Multipair two-way full-duplex relaying with massive array and power allocation," *IEEE Transactions on Vehicular Technology*, vol. PP, no. 99, pp. 1–1, 2017.

[11] B. Xia, C. Li, and Q. Jiang, "Outage performance analysis of multi-user selection for two-way full-duplex relay systems," *IEEE Communications Letters*, vol. 21, no. 4, pp. 933–936, 2017.

[12] C. Li, H. Wang, Y. Yao, Z. Chen, X. Li, and S. Zhang, "Outage performance of the full-duplex two-way df relay system under imperfect csi," *IEEE Access*, vol. 5, pp. 5425–5435, 2017.

[13] L. Li, C. Dong, L. Wang, and L. Hanzo, "Spectral-efficient bidirectional decode-and-forward relaying for full-duplex communication," *IEEE Transactions on Vehicular Technology*, vol. 65, no. 9, pp. 7010–7020, Sept 2016.

[14] B. Zhong and Z. Zhang, "Secure full-duplex two-way relaying networks with optimal relay selection," *IEEE Communications Letters*, vol. 21, no. 5, pp. 1123–1126, May 2017.

[15] G. Chen, P. Xiao, J. R. Kelly, B. Li, and R. Tafazolli, "Full-duplex wireless-powered relay in two way cooperative networks," *IEEE Access*, vol. 5, pp. 1548–1558, 2017.

[16] G. J. Gonzalez, F. H. Gregorio, J. E. Cousseau, T. Riihonen, and R. Wichman, "Full-duplex amplify-and-forward relays with optimized transmission power under imperfect transceiver electronics," *EURASIP Journal on Wireless Communications and Networking*, 2017.

[17] E. Bjornson, M. Matthaiou, and M. Debbah, "A new look at dual-hop relaying: Performance limits with hardware impairments," *IEEE Transactions on Communications*, vol. 61, no. 11, pp. 4512–4525, 2013.

[18] K. Guo, B. Zhang, Y. Huang, and D. Guo, "Outage analysis of multi-relay networks with hardware impairments using secps scheduling scheme in shadowed-rician channel," *IEEE Access*, vol. 5, pp. 5113–5120, 2017.

[19] C. Li, B. Xia, S. Shao, Z. Chen, and Y. Tang, "Multi-user scheduling of the full-duplex enabled two-way relay systems," *IEEE Transactions on Wireless Communications*, vol. 16, no. 2, pp. 1094–1106, Feb 2017.